Citation: Molecular Therapy—Nucleic Acids (2015) 4, e228; doi:10.1038/mtna.2015.1

www.nature.com/mtna

High-affinity RNA Aptamers Against the HIV-1 Protease Inhibit Both *In Vitro* Protease Activity and Late Events of Viral Replication

Sonald Duclair[1], Archana Gautam[1], Andrew Ellington[2] and Vinayaka R Prasad[1]

HIV-1 aspartyl protease (PR) plays a key role in virion morphogenesis, underscoring the effectiveness of protease inhibitors (PI). Despite their utility, side effects and drug-resistance remains a problem. We report the development of RNA aptamers as inhibitors of HIV-1 PR for potential use in anti-HIV gene therapy. Employing Systematic Evolution of Ligands by Exponential Enrichment (SELEX), we isolated four unique families of anti-HIV-1 PR RNA aptamers displaying moderate binding affinities (K_d = 92–140 nmol/l) and anti-PR inhibitory activity (K_is = 138–647 nmol/l). Second-generation RNA aptamers selected from partially randomized pools based on two of the aptamer sequences displayed striking enhancements in binding (K_ds = 2–22 nmol/l) and inhibition (K_is = 31–49 nmol/l). The aptamers were specific in that they did not bind either the related HIV-2 protease, or the cellular aspartyl protease, Cathepsin D. Site-directed mutagenesis of a second-generation aptamer to probe the predicted secondary structure indicated that the stem-loops SL2 and SL3 and the stem P1 were essential for binding and that only the 3'-most 17 nucleotides were dispensable. Anti-PR aptamers inhibited HIV replication *in vitro* and the degree of inhibition was higher for second-generation aptamers with greater affinity and the inhibition was abrogated for a nonbinding aptamer variant.

Molecular Therapy—Nucleic Acids (2015) **4**, e228; doi:10.1038/mtna.2015.1; published online 17 February 2015
Subject Category: Non-coding RNAs

Introduction

The human immunodeficiency virus (HIV) must successfully complete several key steps in its life cycle in order to replicate in the host environment. One such critical step involves the processing of its Gag and Gag-Pol polyprotein precursors into their mature functional components during viral maturation.[1,2] This function is provided by the virally encoded aspartyl protease (PR) and is thought to occur either during or immediately after budding.[3,4] In its active form, PR is a 22 kDa homodimer consisting of two 99-amino acid subunits each contributing a catalytic aspartate residue to the active site.

Over the past two decades, nearly a dozen protease inhibitors (PIs) have been approved by the Food and Drug Administration that can inhibit the proteolytic activity of PR, leading to the production of immature and noninfectious particles.[5,6] These drugs most commonly mimic the natural substrate of PR and work by binding at its active site to prevent substrate binding.[7,8] When used in combination with drugs inhibiting other key steps of HIV replication in highly active antiretroviral therapy, these antiretrovirals can severely reduce viral loads, delay the onset of acquired immune deficiency syndrome (AIDS), and lead to decline in both morbidity and mortality rates among HIV-infected individuals.[9,10] However, a major limitation to their clinical use is the emergence of drug-resistant strains that can replicate in the presence of the PIs,[11] fueling the search for novel compounds.

The numerous crystal structures and nuclear magnetic resonance structures of HIV-1 PR alone as well as PR complexed with substrates and inhibitors have revealed several potential inhibitory sites, including the dimerization interface that is formed between the two subunits as well as the flexible flaps that undergo conformational changes upon substrate binding. The dimerization interface contributes close to 75% of the stabilizing force in the homodimeric PR[12] and is highly conserved among HIV-1 isolates and drug-resistant strains.[13] Several groups have successfully targeted this site in order to interfere with the formation and stability of the functional homodimeric PR.[14–16] Additional inhibitory sites may yet exist on the surface of the protease that may be revealed via the use of RNA aptamers.

RNA aptamers are high-affinity nucleic acid ligands that are isolated through an *in vitro* selection process known as Systematic Evolution of Ligands by Exponential Enrichment (SELEX).[17,18] They form various three-dimensional structures to bind their targets with high affinity and specificity. A number of aptamers have been developed against HIV-1 viral proteins that target key stages of the HIV viral life cycle including enzymatic functions (reverse transcriptase, RNase H, integrase),[19–21] regulation of gene expression (tat/TAR, rev/RRE),[22–25] virus assembly (Gag, nucleocapsid NCp7),[26–28] and viral entry (gp120).[29,30] Although aptamers targeting hepatitis C virus NS3 protease have been described[31] and anti-protease aptamers against clotting factors have proven to be therapeutically useful,[32] none exists that targets the aspartyl protease of HIV-1.

Aptamers targeting HIV-1 proteins have been expressed intracellularly to inhibit HIV-1 replication. Previously, we and others showed that intracellular expression of aptamers targeted to HIV-1 (RT, TAR and Gag) can bring about potent suppression of HIV-1 replication.[26,33–38]

[1]Department of Microbiology and Immunology, Albert Einstein College of Medicine, Bronx, New York, USA; [2]Department of Chemistry and Biochemistry, University of Texas at Austin, Austin, Texas, USA Correspondence: Vinayaka R Prasad, Department of Microbiology and Immunology, Albert Einstein College of Medicine, 1300 Morris Park Ave, Golding 401, Bronx, NY, USA. E-mail: vinayaka.prasad@einstein.yu.edu
Keywords: anti-HIV-1 gene therapy; HIV-1 inhibitor; HIV-1 PR inhibitor; RNA aptamer structure; RNA aptamer
Received 10 October 2014; accepted 1 December 2014; published online 17 February 2015. doi:10.1038/mtna.2015.1

RNA aptamers can potentially be of use in anti-HIV gene therapy in which hematopoietic stem cells that serve as precursors to HIV-1 susceptible cells are engineered to be resistant to viral infections or unsuitable for viral replication.[39,40] In this approach, genes or gene products that confer protection against HIV are delivered into hematopoietic stem cells, which can differentiate into CD4+ T-cells and macrophages, resulting in the regeneration of the hematopoiesis with cells that are protected from the pathogenic effects of the virus. Alternatively, peripheral CD4+ T-cells from HIV-infected individuals may be harvested and transduced *ex vivo* to express the protective genes and reintroduced into the patients. There are a number of completed and ongoing clinical trials utilizing antisense RNAs, ribozymes, siRNAs, and zinc-finger nucleases as inhibitory agents in this approach.[41–44] The advancement in anti-HIV gene therapy is exemplified by a recent report in which a zinc finger nuclease targeting CCR5, a gene that encodes the coreceptor essential for HIV infection, was engineered into peripheral T cells of 12 HIV-infected individuals followed by reinfusion of gene-modified cells. This effort led to gene modification in 13.9% of circulating cells and resulted in the reduction of viremia in most patients including undetectable HIV in one of four patients who could be evaluated.[44] Anti-HIV gene therapy can address many of the limitations of highly active antiretroviral therapy and has the potential to suppress viral replication and preserve the immune system.

We report here, for the first time, the isolation of RNA aptamers targeted to the HIV-1 PR. We describe the initial characterization of their binding affinities, binding specificities, secondary structures, and the nature of the inhibition of HIV-1 protease. We also developed second-generation aptamers with further enhanced binding and inhibition of HIV-1 PR. Mutational analysis of a selected second-generation anti-PR aptamer revealed that most of the aptamer was essential for binding except the 3'-terminal 17 nucleotides. Our results show that the anti-PR aptamers inhibit HIV replication, inhibition is correlated to PR-binding by aptamer *in vitro* and that by employing partially randomized (doped) selections, it is possible to improve the degree of inhibition of virus replication.

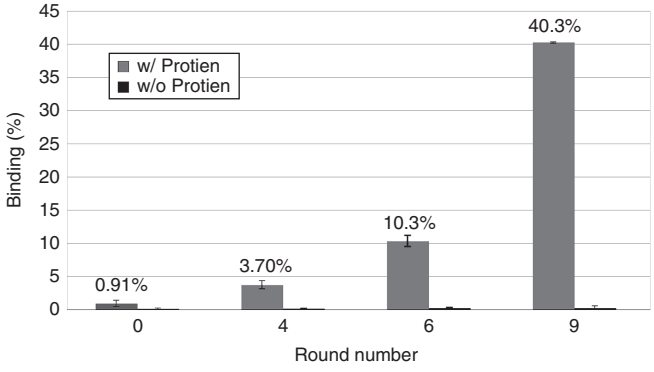

Figure 1 Progress of HIV-1 protease aptamer selections. Internally, ^{32}P-labeled RNAs from the starting library and from pools obtained from round 4, 6, and 9 of the selections were assayed for their ability to bind HIV-1 PR as described in the text. Error bars represent mean ± SD.

Results

Selection and identification of RNA aptamers that bind HIV-1 PR

SELEX was used to identify RNA aptamers that can selectively bind to the recombinant wild-type HIV-1 PR from a previously characterized RNA library with a complexity of 10^{14} unique species.[45] This complexity represents the total number of molecules originally synthesized, and not the full potential complexity of the library. **Figure 1** shows the progress in the improvement of binding through nine rounds of SELEX, monitored via a double filter-binding assay, at selection rounds 4, 6, and 9. Binding assays were performed both in the presence and absence of protein to evaluate the level of nitrocellulose filter binding species present in the pools. Enrichment for protease-binding species was observed as early as the fourth round of selection, which displayed a total binding of 3.7% when compared to the initial starting pool (0.91%) and the samples that did not contain any protease (0.12%). The round 9 pool displayed a total binding of 40%, fourfold higher than the round 6 pool (**Figure 1**). These results indicated that this pool represented an enrichment of RNA species capable of binding the HIV-1 protease.

In order to determine the composition of the selected pool, 48 clones from the 10th round of selection were subjected to sequencing. The individual sequences were aligned and four distinct sequence families were observed (**Table 1**). The PR10.1 was the most abundant family and accounted for nearly 73% of all the sequenced clones. The PR10.9, PR10.13, and PR10.18 families account for 10.4, 6.3, and 4.2% of the clones, respectively. A representative of each aptamer family was selected for determination of dissociation constants. All of the anti-PR aptamers had moderate and comparable binding affinities with K_ds ranging from 93 to 154 nmol/l (**Table 2**). The most abundant PR10.1 aptamer, which accounted for over 70% of the clones, displayed a K_d of 115 nmol/l.

Anti-PR RNA aptamers inhibit HIV-1 protease activity

In order to determine if the RNA aptamers were able to inhibit the enzymatic activity of HIV-1 protease, we employed a FRET-based assay to monitor the rate of substrate cleavage at multiple substrate concentrations and increasing aptamer

Table 1 Sequences of first-generation anti-PR RNA aptamers

RNA	Random sequences (5′-3′)	Frequency (48 clones)
PR10.1	CTTCATTGTAACTTCTCATAATTTCCCGAGGC TTTTACTTTCGGGGTCCT	35 (72.9%)
PR10.9	ACATTACCTAAGTAAGATTACGGCTTCGAG TTTAGAGACCTCTCCCTGGT	5 (10.4%)
PR10.13	CCGGGTCGTCCCCTACGGGGACCTAAAGAC TGTGTCCAACCGCCCTCGCCT	3 (6.3%)
PR10.18	TCAGACATTTACCTCACTTCGTCTGTTCAAT CGGGTAACACTCGGGATGA	2 (4.2%)
Others	Orphan sequence	3 (6.3%)

Alignment of the 48 clones after 10 rounds of SELEX revealed four distinct sequence families with no sequence homology between the families. Only the variable region sequences of the aptamers (5′-3′) are shown. Frequencies of occurrence are given as percentage (%).

Table 2 Dissociation and inhibitory constants of first- and second-generation anti-PR RNA aptamers

Aptamer	K_d (nmol/l)	K_i (nmol/l)
PR10.1	115±22	254±39
PR10.9	93±19	301±34
PR10.13	154±13	138±24
PR10.18	140±17	864±66
PR10.1-8A	2.2±0.2	31.5±2
PR10.1-8E	17±3	35.6±1
PR10.9-8E	22±9	48.8±2
PR10.9-8N	4.3±0.2	35.5±1

Internally, ^{32}P-labeled representatives of each aptamer family were incubated with increasing amounts of HIV-1 PR and a percentage of RNA bound to protein was measured at each concentration as described in the text. The dissociation constants (K_d) were then determined from the percentage of RNA bound at the various protein concentrations. The rate of cleavage of an HIV-1 PR FRET substrate was measured over a wide range of aptamer and substrate concentrations. The K_is were determined from non-linear regression globally fit to the equation for noncompetitive inhibition using Prism.

concentrations to determine inhibitory constants for the RNA aptamers (**Table 2**). All four aptamers were tested for their ability to inhibit HIV-1 protease. The best inhibitory aptamer, PR10.13, had a K_d of 154 nmol/l. Although only three individuals of this family were identified in the selected aptamer pool, this aptamer had a K_i of 138 nmol/l, which is a little over twofold higher than the homodimeric PR concentration in our assays suggesting potent inhibition (**Table 2**). Interestingly, although the PR10.13 aptamer was the best inhibitor it was not the species with the highest affinity for HIV-1 PR and it had a K_i that was 2.2-fold lower than that of the best binder, the PR10.9 aptamer. In order to determine the mode of inhibition, a Lineweaver-Burk plot was generated for the PR10.13 aptamer (**Supplementary Figure S1**). The *x*-intercept which represents the inverse of the K_m did not vary for the different aptamer concentrations, consistent with a noncompetitive inhibition.

RNA aptamers compete with each other for PR-binding site

As previously mentioned, the four sequence families of RNA aptamers isolated from the selections are very distinct. They do not share any sequence homology and no common secondary structural motifs were detected from the predicted secondary structures generated by free energy minimization using the RNA folding algorithm Mfold (data not shown).[46] In order to determine if these aptamers bind to the same or different sites on PR, we conducted a competition binding assay by incubating PR with internally α-^{32}P-radiolabeled PR10.1 RNA aptamer in the presence or absence of increasing amounts of excess nonradiolabeled competitor RNA and comparing the binding affinities. The PR and radiolabeled RNA concentrations were kept constant in these binding assays to isolate the effect of the competitor. The competitor concentration was varied and ranged from 33 nmol/l to 1 µmol/l (10-fold excess over the protein concentration). In order to determine if this experimental set up could accurately detect competition for binding sites on PR, we used excess nonradiolabeled competitor of the same species as a positive control and the

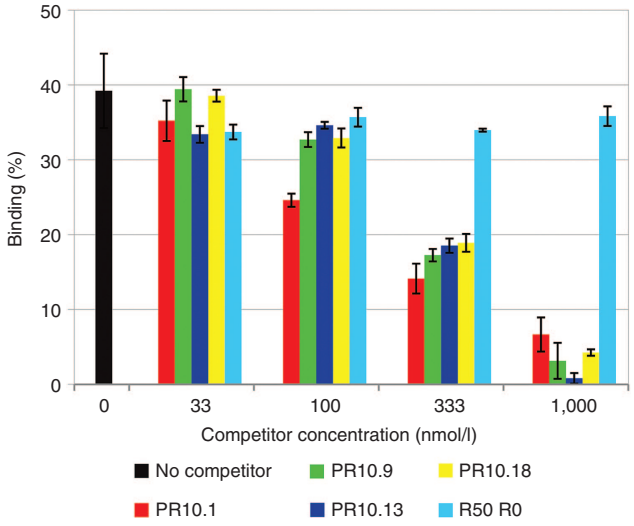

Figure 2 Competition binding assay between different RNA aptamer families. Internally, ^{32}P-labeled PR10.1 RNA aptamer was allowed to bind to HIV-1 PR that was preincubated with increasing amounts of the indicated competitor and the percentage of bound radiolabeled RNA was measured at the various competitor concentrations. RNA aptamers from different families, sharing little sequence or structure homology, compete for PR binding. Error bars represent mean ± SD.

starting RNA library, which has very little affinity for PR, as a negative control. When the same aptamer species is used as the cold competitor, binding was severely reduced compared to no competitor control, and when the starting RNA library was used, binding was only mildly affected at the highest concentration tested (**Figure 2**), thus indicating that our competition binding assay can be used to monitor the binding of PR binding sites with excess competitor. Interestingly, binding to PR by the PR10.1 can be competed out by the PR10.9, PR10.13, and PR10.18 RNA aptamers despite the fact that these aptamers do not share any common structural features. These results indicated that the aptamers are either binding PR at the same site, overlapping sites or adjacent sites that are so closely located relative to each other that one binding event prohibits the binding of another aptamer. It is also possible that aptamer binding may induce conformational changes in non-adjacent domains that are required for binding.

Selection of PR RNA aptamers with enhanced binding affinities

The binding affinities of the first-generation RNA aptamers were relatively low and hence, we sought to improve them by isolating variants from newly generated doped pools of selected aptamers. The PR10.1 and PR10.9 RNA aptamers were chosen for doping and further selection. Doped pools were generated starting with the above sequences with 20% mutations at each position across the variable 50-nucleotide region. The doped pools were used as starting material for an additional eight rounds of selection and several variants were identified in the selected round 8 pools of the PR10.1 and PR10.9 RNA aptamers (**Table 3**). The pools were sequenced at round 3 and round 8. Two representative aptamers from

Table 3 Sequences of second-generation PR10.1 and PR10.9 RNA aptamers

RNA	Parent	Aptamer sequences (5′-3′)
PR10.1	N/A	CTTCATTGTAACTTCTCATAATTTCCCGAGGCTTTTACTTTCGGGGT_CCT
PR10.1-8A	PR10.1	CTTAAGTGTAACTTCTCGTAATT_CCCAAGGCTTTTAC_CTCGGGGT_CCT
PR10.1-8C	PR10.1	CTTAAGTGTAACTTCTCGTAATT_CCCAAGGCTTTTAC_CTCGGGGT_CCT
PR10.1-8T	PR10.1	CTTAAGTGTAACTTCTCATAATT_CCGAAGGCTTTTACTTTCGGGG__CCT
PR10.1-8D	PR10.1	CTTAAGTGTAACTTCTCCTAACATCCGGAGGCTTTTACTTCCGGGGA_CCT
PR10.1-8E	PR10.1	CTTAAGTGTAACTTCTCATAACATCCGGAGGCTTTTACTTCCGGGGA_CCT
PR10.1-8M	PR10.1	CTTAAGTGTAACTTCTCCTAACATCCGGAGGCTTTTACTTTCGGGGA_CCT
PR10.1-8S	PR10.1	CTTAAGTGTAACTTCTCCTAACATCCCGAGGCTTTTAC_TTCGGGGGACCT
PR10.1-8Q	PR10.1	TTTAAGTGTAACTTTTCATAACTACCCGACGCTTTTACGTTCGGGGG_CCT
PR10.1-8O	PR10.1	CTTCAGTGTAACTTCTCATAACATCCGAAAGCTTTTACTGTCGGGGA_CCT
PR10.1-8P	PR10.1	CTTCAATGTAACTTCTCCTAAT_TCCCAAAGCTTTTACTTTCGGG_T_CCT
PR10.9	N/A	ACATTACCTAA_GTAAGATTACGGCTTCGAGTTTAGAGACCTCTCCCTGGT
PR10.9-8C	PR10.9	ACATTACCTAAGGTAAGATAACGGCTTCATGTTTAGAGACCCCTCCCTGGT
PR10.9-8R	PR10.9	ACATTACCTAAGGTAAGATAACGGCTTCATGTTTAGAGACCTCTCCCTGGT
PR10.9-8K	PR10.9	ACATTACCTAAGGTAAGATAACGGCTTCACGTTCAGAGACCTCTCCCTGGT
PR10.9-8E	PR10.9	ACATTACCTA_GGTAAGATAACGGCTTCGCGTTCAGAGACCTCTCCCTGGT
PR10.9-8L	PR10.9	ACATTACCTAAGGTAAGATAACGGCTTCTAGTTCAGAGACCTCTCCCTGGT
PR10.9-8H	PR10.9	ACATTACCTAAGGTAGGAATACGGCTTC_GGTTCAGAGACCTCTCCCTGGT
PR10.9-8N	PR10.9	__TTGACCTAAGGTAAGATAACGGCTTCGAGTTCAGAGACCTCGCCCTGGT
PR10.9-8Q	PR10.9	__TTGACCTAAGGTAAGATAACGGCTTCGAGTTCAGAGACCTCGCCCTGGT

The round 8 pools from the doped PR10.1 and PR10.9 selections were cloned and sequenced. Aptamer sequences shown exclude the flanking constant sequences. Substituted residues are underlined.

the round 8 pools of PR10.1 and PR10.9 were selected for determination of dissociation constants (**Table 2**). The second-generation PR RNA aptamers, PR10.1-8A, PR10.1-8E, PR10.9-8E, and PR10.9-8N bound PR with significantly higher affinities with K_ds of 2.2, 17, 22, and 4.3 nmol/l respectively (**Table 2**). In the case of the PR10.1-8A, this enhancement corresponded to a 52-fold increase in binding affinity. The doped aptamers also exhibited enhanced efficacy in inhibiting the activity of PR compared to the parental sequences with K_is ranging from 31.5 to 48.8 nmol/l (**Table 2**). Thus, the inhibitory constants of the PR10.1 and PR10.9 aptamers were improved by ~8- and 8.5-folds, respectively. As expected, these second-generation anti-PR RNA aptamers were also found to be noncompetitive as they did not compete with the substrate, suggesting that they are binding to a site other than the active site (**Supplementary Figure S1**).

Mutational analysis of a second-generation PR10.1-8E RNA aptamer to map structural elements important for PR binding

The enhancements in binding affinities and inhibitory potencies observed with the second-generation RNA aptamers were accompanied by, on average, six to seven substitutions in the parental sequences (**Figure 3a**). We used Mfold[46] to predict their secondary structures, determine whether a minimal structure was sufficient for PR-binding and to map the regions that may have been altered to enhance binding. Several of the substitutions in the doped aptamers derived from the PR10.1 aptamer mapped to the two stem-loops (SL2 and SL3) that are predicted to form in both the parental and derivative aptamers (**Figure 4a**,**b**). The size of the SL3 loop in this region is predicted to be shorter in length by 1 base in both the PR10.1-8A and PR10.1-8E aptamers. In order to determine the role played by this predicted stem-loop in PR binding and whether its formation is required for binding we created a set of mutations (DSL3, M1, M2, and M3) in this region as depicted in **Figure 3b**. Binding was abolished when the entire SL3 stem-loop was deleted (PR10.1-8E-DSL3), when the loop (5′-CUUUUA-3′ to 5′-CACGUA-3′; PR10.1-8E-M1) or one of the strands in the stem were mutated (5′-CUUCCGGG-3′ to 5′-GAAGGCCC-3′; PR10.1- 8E-M2) (**Figure 3c**). Binding was restored when complementary mutations were introduced in both stems to re-establish base pairing (5′-UCCGGAGG-3′ to 5′-GGGCCUUC-3′; PR10.1-8E-M3) albeit with a different sequence, indicating that both the loop sequence and the stem base-pairing are required for binding.

However, the PR10.1-8E-M3 mutant, which has a K_d of 60.0 nmol/l (**Supplementary Table S2**) bound PR less tightly than the PR10.1-8E aptamer (K_d = 17±3 nmol/l) but more tightly than the first-generation PR10.1 aptamer (K_d = 115±22 nmol/l).

The effect of the SL2 stem-loop on PR binding was tested via a second set of mutants (DSL2, M4, M5, M6, and M8). Deletion of this entire region as in the PR10.1-8E-DSL2 mutant abolished PR binding. Similarly, mutations in either strands that were intended to perturb base pairing of S2 as in the PR10.1-8E-M5 (from 5′-ATGCT-3′ to 5′-TACGA-3′) and PR10.1-8E-M6 (from 5′-AGTGT-3′ to 5′-TCACA-3′) mutants, or mutations in the L2 loop as in the PR10.1-8E-M4

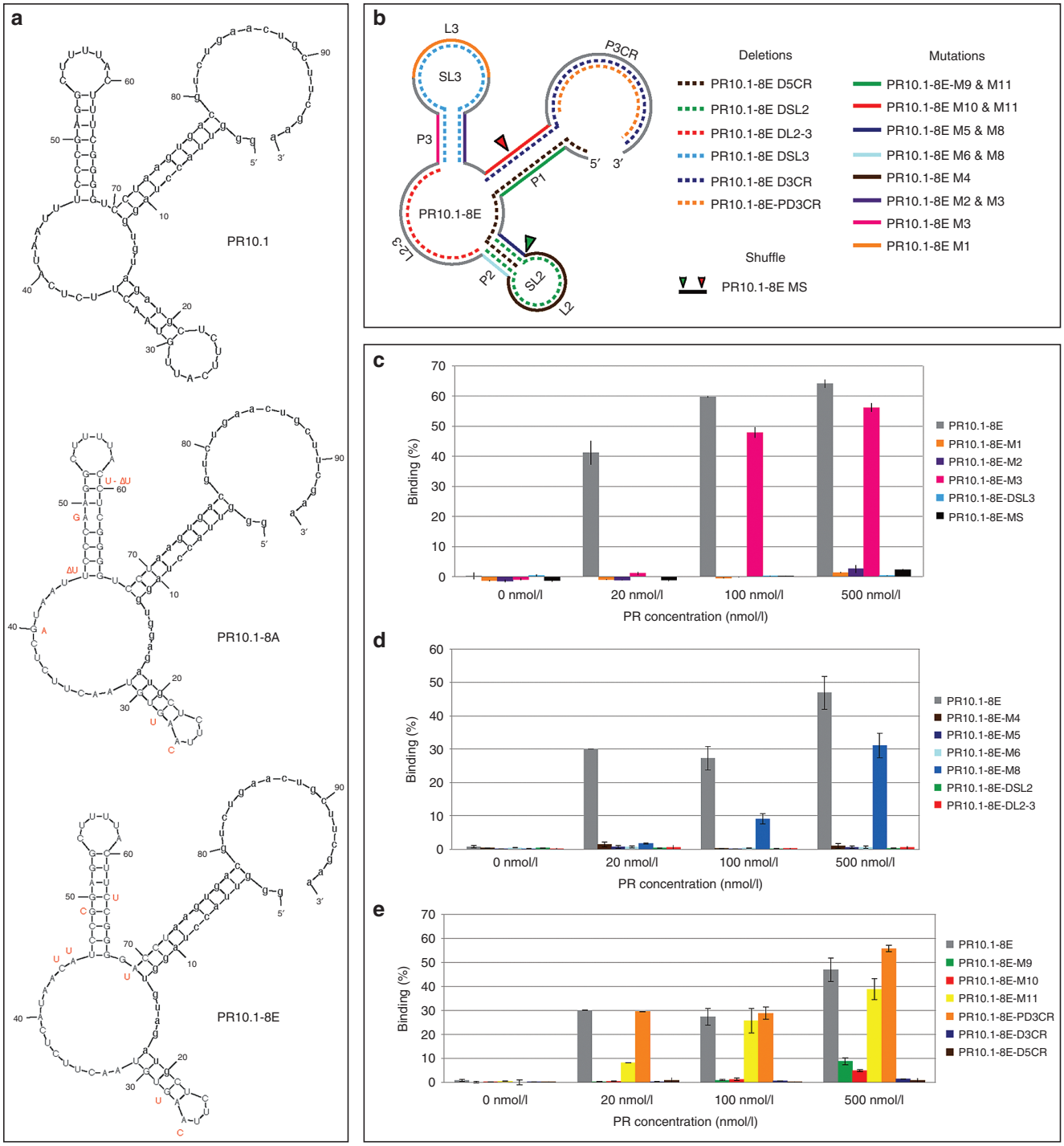

Figure 3 Mutational analysis of second-generation aptamer, PR10.1-8E. (**a**) Structure predictions. Mfold was used to predict the secondary structures of the first-generation aptamer PR10.1 and the second-generation aptamers PR10.1-8A and PR10.1-8E to map substitutions that enhanced PR binding. The substitutions and deletions compared to the PR10.1 aptamer are indicated in red (for precise positions of substitutions and deletions, the reader is referred to Results section). The 5′- and 3′-constant regions are shown in lower case. (**b**) Schematic representation of PR10.1-8E mutants tested for PR binding. The outer solid grey line represents the unmodified PR10.1-8E aptamer. The solid colored lines indicate regions that are mutated in the corresponding aptamers. The inner broken lines indicate regions that are deleted in the corresponding aptamers. The green arrowhead marks the end of the 5' constant region and the start of the random region. The red arrowhead marks the end of the random region and the start of the 3′ constant region. The random region is shuffled in the PR10.1-8E-MS mutant. (**c–e**) Binding assays with various mutants. Internally, ^{32}P-labeled mutant aptamers were assayed for PR binding with increasing amounts of PR. The aptamer mutants PR10.1-8E-M3 (**c**), PR10.1-8E-M8 (**d**), PR10.1-8E-M11 and PR10.1-8E-PD3CR (**e**) retained their ability to bind PR. Error bars represent mean ± SD. The colors for shading of the bars representing the combined mutation of both strands, M8 and M11 have been chosen to distinguish them from mutation in each strand of the corresponding stem.

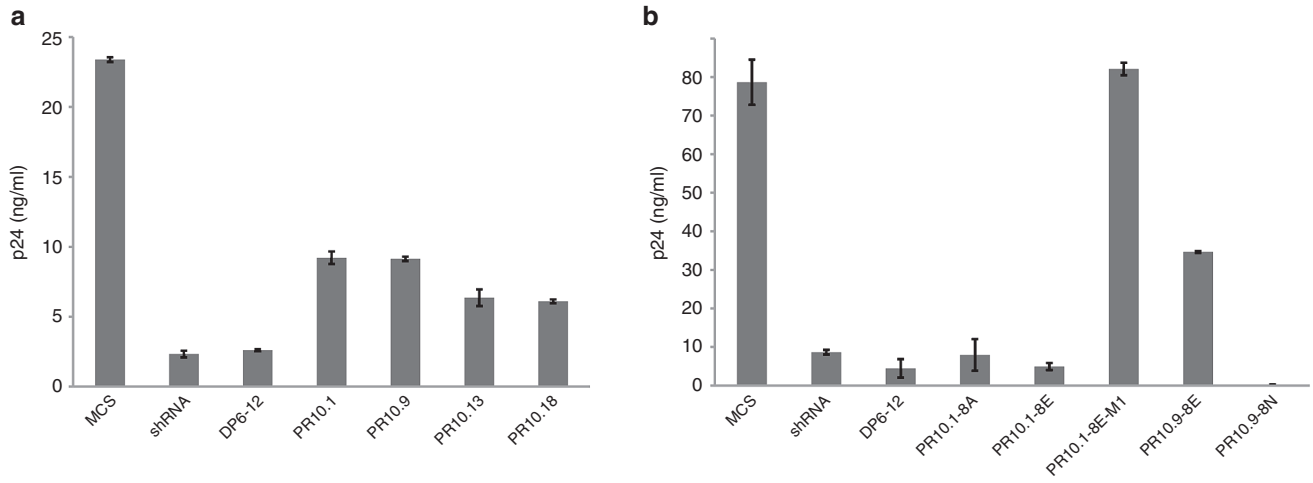

Figure 4 Effect of anti-PR aptamers on HIV-1 virus production. The effect of anti-PR aptamers on virus production was assessed using HEK 293T cells cotransfected with pNL4-3.Luc/pVSV-G along with various control or aptamer-encoding pSilencer plasmids. Virus-containing supernatants were harvested 48 hours post-transfection and P24 enzyme-linked immunosorbent assays were performed to monitor the amount of virus released (reported here as nanogram of p24 per milliliter of culture supernatant). (**a**) Effect of first-generation aptamers on viral production. The expression of first-generation anti-PR aptamers inhibited the release of virus-associated p24 by ~60–73%, compared to the positive controls, Tat/Rev shRNA and DP6-12 aptamer, that exhibited ~90% inhibition. (**b**) Effect of second-generation aptamers on viral production. Enhanced inhibition of viral production was observed with the second-generation anti-PR aptamers. The PR10.1-8A and PR10.1-8E aptamers both displayed inhibition comparable to the positive controls, while the mutant PR10.1-8E-M1 aptamer, which does not bind to PR, had no effect on particle release. The greatest inhibition observed was associated with PR10.9-8N aptamer, which generated a reading that was below the detection level (not dectected). Error bars represent mean ± SD.

mutant (from 5′-CTTA-3′ to 5′-ACGT-3′) also abolished PR binding (**Figure 3d**). Attempts to restore P2 base-pairing via complementary mutations in both strands (from 5′-ATGCT-3′ and 5′-AGTGT-3′ to 5′-TGTGA-3′ and 5′-TCGTA-3′ respectively; PR10.1-8E-M8) also re-established some PR binding, although it was significantly less than either the second-generation PR10.1-8E aptamer or the original PR10.1 aptamer. This mutant has a K_d of 386 nmol/l (see **Supplementary Table S2**).

The secondary structures predicted by Mfold[46] also indicated that the 5′-constant region and part of the 3′-constant regions would form the P1 stem, which appears to be stabilizing the overall conformation of the first and second-generation PR10.1 RNA aptamers. In order to determine if the corresponding residues are required for PR binding, several mutations were created. In the PR10.1-8E-D5CR mutant, the entire 5′ constant region was deleted. In the PR10.1-8E-D3CR mutant, the residues downstream of the SL3 stem-loop, including the entire 3′ constant region and four nucleotides immediately upstream of it, were deleted, whereas only the residues in the 3′ constant region that were predicted not to form any interactions with the remainder of the aptamer were deleted in the PR10.1-8E-PD3CR mutant (**Figure 3b**). In addition, we also created the PR10.1-8E-M9 mutant (from 5′-GUUACCUAGGU-3′ to 5′-CAGUGGAUCCA-3′) and PR10.1-8E-M10 mutant (from 5′-ACCUAAGUGAC-3′ to 5′-UGGAUCCAUUG-3′) that abolished base pairing in the P1 stem and PR10.1-8E-M11 mutant containing complementary mutations in both strands of the P1 stem to test the requirement for base pairing in this region. The PR10.1-8E-D5CR, PR10.1-8E-D3CR, PR10.1-8E-M9, and PR10.1-8E-M10 mutants all failed to bind PR to any appreciable extent even at the highest concentrations tested. However, when complementary mutations were introduced (PR10.1-8E-M11) to restore base pairing, PR binding was also restored (**Figure 3e**). This is an indication that base-pairing in this region is important for PR binding. Interestingly, the PR10.1-8E-PD3CR mutant, which lacks the last 17 residues of the 3′ constant region downstream of the P1 stem did not lose its ability to bind PR. In fact, this mutant bound PR more efficiently than the PR10.1-8E with a K_d of 1.7 nmol/l (see **Supplementary Table S2**), thus indicating that these residues are not critical for PR-binding, as their omission do not significantly affect PR binding but rather enhances it.

Other mutations studied for PR binding include the PR10.1-8E-DL2-3 mutant where 11 residues between the SL2 and SL3 stem-loops were deleted and the PR10.1-8E-MS mutant where the entire variable region sequence was randomized. Neither the PR10.1-8E-DL2-3 mutant nor the PR10.1-8E-MS mutant displayed any PR binding at any concentration (**Figure 3c**,**d**).

Specificity of anti-PR RNA aptamers

HIV-1 PR is encapsidated into the budding virion as a part of the Gag-Pol polyprotein and it exerts its proteolytic function during viral maturation. Thus, the newly isolated anti-PR RNA aptamers would be most effective if they are able to interact with PR during or prior to viral assembly and are therefore intended to be used as intracellular aptamers, to be expressed in HIV-susceptible cells. Although aptamers are known for their exquisite specificities, intracellularly expressed anti-PR RNA aptamers may cause adverse effects if they are able to interact with cellular aspartyl proteases. The cellular aspartyl protease, cathepsin D, is ubiquitously expressed in the lysosome and is known to play a major role in apoptosis.[47] In order to assess the specificities

of the anti-PR RNA aptamers and determine if they are able to interact with cathepsin D, we tested their ability to inhibit its function in vitro. In addition, we also tested their ability to bind to the related HIV-2 protease (39 identical out of 99 residues[13]). The anti-PR aptamers did not bind to cathepsin D nor did they inhibit its enzymatic activity at the highest tested concentration of 1 µmol/l (**Supplementary Figure S2a,b**). Furthermore, they did not bind to the PR of the related lentivirus HIV-2, thus indicating specificity.

Effects of anti-PR RNA aptamers on viral production

In order to determine the effects of anti-PR RNA aptamers on viral replication, a cotransfection scheme was employed to generate viral particles in the presence and absence of the aptamers. We cotransfected HEK 293T cells with pNL4-3.Luc[48] and pVSV-G along with pSilencer plasmids that would express the various first and second generation anti-PR aptamers as well as control vectors, including the well-characterized Tat/Rev shRNA[49,50] and the DP6-12 Gag aptamer,[26] both of which have previously been shown to be efficacious in transient transfection experiments. The aptamer sequences were flanked by self-cleaving hammerhead ribozyme to eliminate post-transcription modifications and ensure proper folding as previously described.[26] We then monitored the effect of the RNA aptamer expression on viral production by measuring the amount of virus-associated capsid protein (p24) released in the culture supernatants via a p24 enzyme-linked immunosorbent assay (**Figure 4**). The expression of first-generation anti-PR aptamers inhibited the release of virus-associated p24 by ~60–73%, compared to empty vector control (Multiple Cloning Site (MCS)). In contrast, the positive controls Tat/Rev shRNA and DP6-12 aptamer exhibited ~90% inhibition. Enhanced inhibition of viral production was observed with the second-generation anti-PR aptamers. The PR10.1-8A and PR10.1-8E aptamers both displayed inhibition comparable to the positive controls. Among the other two second-generation aptamers, PR10.9-8E aptamer had no improvement from its parent aptamer in its inhibition of particle release, while PR10.9-8N had the greatest inhibition, generating a reading that was below the detection level. The mutant PR10.1-8E-M1 aptamer, which does not bind to PR, had no effect on particle release showing that the inhibition is mediated by PR-binding.

Discussion

The anti-PR RNA aptamers described here represent a unique class of inhibitors against HIV-1 PR. They bind PR with high affinity and specificity and they are able to inhibit its proteolytic activities noncompetitively. The location on the PR surface where these aptamers are binding remains unknown. However, inhibitory allosteric binding sites have indeed been described for other PR inhibitors.[51,52] One such potential allosteric site is located at the elbow region at the base of each of the glycine-rich β-hairpin flaps and another at the dimerization interface that is formed between the β-sheets of the two subunits. As evident from the numerous crystal and NMR structures,[53–55] PR can adopt three different conformations, including an open, a semiopen and a closed conformation.[52] Upon substrate binding, PR changes to the closed conformation.[56–58] It has been proposed that an inhibitor that can bind to these allosteric binding sites may affect the flexibility of protease to adopt to these different conformations and disrupt its functions, effectively inhibiting the protease.[52] Indeed, several compounds have been identified that inhibit PR noncompetitively and that have been proposed to bind to these allosteric sites.[59,60] A compound that efficiently inhibited PR that was initially designed to prevent protease dimerization did not actually disrupt the dimer interface but rather acted allosterically by binding at this region.[59] Monoclonal antibodies[60] (mAbs) that were developed against PR and potently inhibited its functions were later shown to be targeting residues at the flap elbow region and the dimer interface. Other potential inhibitory allosteric sites may yet exist. In the case of our aptamers, at this point, the locations where they bind on the PR protein remain unclear. Our current study only indicates that they are not binding to the active site, as they do not compete with the substrate. Moreover, the hydrophobic residues surrounding the active site are unlikely to be conducive for binding of the negatively charged RNA aptamer. Surface charge analysis has previously revealed clusters of positively charged residues on PR[61] that would form more favorable interactions with the aptamers. Coincidently, one of these clusters is located at the hinge region of the flap, which has been suggested to be an inhibitory allosteric site. This cluster is a representation of the underlying positive side chains of Lysine 41, Lysine 43, Lysine 45, and Lysine 55. Two other clusters formed by Histidine 69 and Lysine 70 as well as Arginine 14 and Lysine 40, may also serve as a potential site for aptamer interactions. Further investigation is required to determine the residues on PR that are crucial for the new binding interaction with the RNA aptamers and determine if those residues overlap with the residues from the above-mentioned allosteric binding sites. The secondary structures predicted by Mfold agreed strongly with the experimental data obtained from the mutational analysis of the PR10.1-8E RNA aptamer. Base-pairing in the regions corresponding to the P1, P2, and P3 stems appear to be required for PR binding as mutations that abolished putative base-pairing also abolished PR binding (**Figure 3c–e**). Moreover, when base pairing was restored in variants with mutations in both strands of the stems in these regions, PR binding was also restored. Minimally, these results indicate that PR binding requires base-pairing in these stem regions and the sequence of these stem regions is less important. In addition, several of the substitutions in the second-generation RNA aptamers that enhance both binding affinities and inhibitory potencies were mapped to the two stem-loops that are predicted to form (**Figure 3a**). The loops in these regions appear to play a role in PR binding as mutations in these regions abolished PR binding. Our data, however, did not address whether the sequences are required for direct binding to PR or for the formation of a pseudoknot by annealing to other single-stranded regions in the aptamer. Although the 5′- and 3′-boundaries of the first- and second-generation PR10.1 RNA aptamers have not been systematically defined, the data presented here suggests that the 5′ constant region and at least a part of the 3′ constant regions are playing a role in PR binding. Moreover, omission of the last 17 residues

of the 3′-constant region that are predicted not to interact with the remainder of the aptamer, did not abolish PR binding but rather enhanced the binding affinity of the aptamer.

Our study on the effects of the anti-PR aptamers on late events of viral replication revealed that they can inhibit virus production when expressed transiently in producer cells. The ability of the aptamers to inhibit HIV late events of replication appears to be directly related to PR-binding *in vitro*. Second-generation anti-PR aptamers with enhanced binding affinities exhibited greater efficacy of inhibition of viral particle release compared to the first-generation aptamers which bind PR *in vitro* with lower afinities. The dramatic reduction in the inhibition by the nonbinding M1 mutant also shows that aptamer-binding to the PR is essential for this inhibition. Thus the variation in inhibition of virus release appears to directly correlate with *in vitro* aptamer binding affinity to PR. The inhibitory effect of anti-PR aptamers indicates that the aptamers likely assume a three-dimensional conformation within the cell and do localize to the cytoplasm. In order to understand whether the reduction in virus release was due to a release defect, we examined the ratio of virion associated p24 to cell-associated p24 levels, which revealed that for all aptamers, the intracellular p24 was also reduced commensurate with the reduction in the extracellular level indicating no change in release efficiency (**Supplementary Figure S3**). We do not know the mechanism by which the anti-PR aptamers interfere with PR to reduce intracellular Gag. Using a selected subset of aptamers, we examined whether the processing of virion proteins was affected by the aptamers, which revealed no major alterations in virion protein processing suggesting no major changes in virion maturation (**Supplementary Figure S4**). We also examined the effect of anti-PR aptamer expression in the producer cells on the infectivity of the progeny virions in TZMbl reporter cells—the effects observed were less than twofold if any (**Supplementary Figure S5**). Further investigation is needed to understand the mechanism by which the anti-PR aptamers reduce the intracellular Gag levels.

Anti-HIV gene therapy using gene-modified T-cells and hematopoietic stem cells is an emerging new approach with the potential to suppress viral replication and address many of the limitations of combination therapy. Although many viral proteins have been targeted using this approach in both human clinical trials and ongoing preclinical studies, HIV-1 protease, a proven therapeutic target, has yet to be targeted in anti-HIV gene therapy. The anti-PR RNA aptamers characterized here have the potential to be utilized in such an approach by intracellular expression to confer resistance to viral replication.

We have reported the isolation and characterization of the first RNA aptamers targeted to the HIV-1 protease. We performed *in vitro* binding studies and FRET studies to determine their binding and inhibitory constants. The anti-PR RNA aptamers inhibit PR in a noncompetitive manner, suggesting binding to a site other than the active site. Second-generation RNA aptamers with enhanced affinities for PR were generated that inhibited the enzyme with greater efficiency. We performed mutation analysis on these doped aptamers to probe for structural elements that are important for PR binding and identified several stem-loops critical for the aptamer-PR interaction. We have also shown that these aptamers can differentiate the HIV-1 PR from the eukaryotic aspartyl protease cathepsin D and from the more closely related HIV-2. Finally, we have demonstrated that the expression of anti-PR aptamer can inhibit HIV replication at a late step of virus release.

Materials and methods

Protein target and pools of RNA sequences. Recombinant wild-type HIV-1 Protease was obtained from the NIBSC Programme EVA Centre for AIDS reagents (UK). This enzyme was provided in 10 mmol/l sodium acetate, 0.05% 2-mercaptoethanol, 1 mmol/l ethylenediaminetetraacetic acid, 20% glycerol, and 5% ethyleneglycol and stored frozen at –80 °C. The R50 RNA pool containing two copies of 10^{14} unique species has been previously characterized.[45] Briefly, the RNA pool consisted of a 50-nt random region flanked by constant regions that are used as primer sequences for amplification. The doped PR10.1, PR10.9, and PR10.13 RNA pools were synthesized to contain 80% WT residues and 20% non-WT residues across the 50-nt random region such that at each position there was an 80% chance that the correct nucleotide would be present and a 20% chance that one of the remaining three nucleotide would be present (6.67% chance each). The newly synthesized doped DNA pools were processed as previously described[62] and transcribed *in vitro* to generate RNA for the first round of doped selections.

In vitro selections. At the start of each round of selection, the RNA pools were denatured in selection buffer (20 mmol/l HEPES pH 7.4, 150 mmol/l NaCl, 5 mmol/l $MgCl_2$) by heating to 70 °C for 10 minutes and allowed to refold by slowly cooling to room temperature. In the first round of selection, 332 pmol (two copies of each species—10^{14} molecules total) of the starting pool was incubated at 37 °C for 30 minutes with 166 pmol of PR (2:1 molar ratio). The protein-RNA complexes were partitioned from unbound RNA via filtration through 0.45 µm nitrocellulose disk (Millipore, Bedford, MA). After washing four times with selection buffer, the bound protein-RNA complexes were eluted twice in 7 mol/l urea by heating to 95 °C for 5 minutes. The recovered RNA was ethanol precipitated and then reverse transcribed using Superscript III reverse transcriptase (Invitrogen, San Diego, CA) and then polymerase chain reaction (PCR) amplified using 41.R50 forward primer 5′-GATAATACGACTCACTATAGGGTTACCTAGGTGT AGATGCT-3′ (T7 promoter underlined) and 24.R50 reverse primer 5′-TTCGAAGCAGTTCAGACGTCACTT-3′. The PCR products were purified by phenol–chloroform extraction and transcribed using Ampliscribe T7 High Yield Transcription Kit (Epicentre, Madison, WI). At the end of the transcription reaction, the DNA templates were digested with DNase I and the remaining RNA transcripts were gel purified on 8% denaturing PAGE and ethanol precipitated. The recovered RNA was quantified via UV spectroscopy using Nanodrop and used for the next round of selection. Negative selections were performed prior to every alternate round of selection by allowing the refolded RNA pools to incubate with crushed pieces of nitrocellulose for 5 minutes at room temperature and then

filtered through three layers of nitrocellulose disk in the absence of protein. The flow-through collected was then used for selection for the next round of SELEX with PR. During the course of the selections, the stringency was increased by either increasing the number and volume of the washes used during partitioning, reducing the concentration of PR in the binding reactions thus increasing the ratio of RNA to protein or introducing an excess amount of yeast tRNA (Sigma Aldrich, St Louis, MO). The volume of the washes was doubled to twofolds of the binding reaction volume (200 µl in total) and the number of washes was increased from four to five for rounds 4–6. The number of washes was increased to 10 total (2× volume each) for rounds 7–9 and the PR concentration was reduced fivefolds to achieve a 10:1 ratio of RNA to protein. Yeast tRNA was also added in 10-fold excess over the RNA concentration in the binding reactions for rounds 7–9. The highest level of stringency was used for the final, 10th round in order to isolate the species with the highest affinity for PR by increasing the ratio of RNA to protein to 20:1. After this round, the pool of RNA was reverse transcribed, converted to double-stranded DNA during PCR amplification and subsequently cloned into the pCR2.1 TOPO vector using the TOPO TA cloning kit (Invitrogen, San Diego, CA) and some of the clones were sequenced (**Table 1**). The doped selections were carried out under similar conditions. Representatives of the doped pools were sequenced at round 3 and round 8 (**Table 3**).

Binding affinities of RNA pools. RNA transcripts that were used for pool binding assays were internally labeled with (α-^{32}P)-UTP (3000 Ci/mmol, 10 mCi/ml, Perkin Elmer, Waltham, MA) during transcription. Internally labeled RNA at a final concentration of 100 nmol/l was incubated with 200 nmol/l of PR for 30 minutes at 37 °C in selection buffer after denaturation and refolding. The binding reactions were sieved through two filters on a vacuum manifold and washed four times with selection buffer to separate the bound RNA-protein complexes from the free RNA. A 0.45 µm nitrocellulose filter (Whatman, Piscataway, NJ) was used on the top layer to capture all of the RNA-protein complexes and the remaining free RNA was captured by the nylon filter (Amersham Biosciences, Pittsburg, PA) at the bottom. Both filters were later dried and visualized via Phosphorimager (GE Healthcare, Piscataway, NJ). The percent binding was then measured by determining the radioactivity retained on the nitrocellulose filter over that collectively retained on the nitrocellulose and the nylon filters (**Figure 1**).

Determination of dissociation constants. RNA transcripts with high specific activities were prepared for binding assays using Maxiscript T7 Transcription Kit (Ambion, Austin, TX) such that one out of every 100 residues of UTP in these transcripts is labeled with α-^{32}P. The binding reactions were carried out by incubating 1 nmol/l of internally labeled RNA with 10, 20, 40, 80, 160, 320, and 640 nmol/l PR for 30 minutes at 37 °C in selection buffer in the presence of excess yeast tRNA. The RNA-protein complexes were partitioned and a percentage binding was measured for each protein concentration as previously described (**Table 2**). The binding assays for the high affinity second-generation RNA aptamers contained 0.1 nmol/l of labeled RNA and 1, 2, 4, 8, 16, 32, and 64 nmol/l PR (**Table 2**). The percentage binding was plotted as a function of protein concentration in accordance with the sigmoidal dose response with variable slope and the dissociation constants were determined using Prism software (Version 4.0a, Graphpad Software, La Jolla, CA).

Competition binding assays. The competition binding reactions were carried out by incubating 100 nmol/l of PR with 33 nmol/l, 100 nmol/l, 333 nmol/l, or 1 µmol/l of competitor RNA for 10 minutes at 37 °C in selection buffer. Following this preincubation period, ^{32}P-labeled PR10.1 aptamer RNA was added to the reaction at a final concentration of 1 nmol/l and incubated for an additional 15 minutes. The binding reactions were later partitioned and a binding percentage was measured for each sample as previously described. The PR10.1 aptamer was tested individually against PR10.1, PR10.9, PR10.13, and PR10.18 as competitors as well as against the initial R50 R0 pool (**Figure 2**). The R50 R0 pool does not bind PR to any appreciable extent and thus served as a negative control. The unlabeled PR10.1 competitor RNA served as a positive control.

HIV-1 protease inhibition assays. Sensolyte 520 HIV-1 Protease assay kit (Anaspec, Fremont, CA) was used to measure the initial velocities of the proteolytic cleavage by PR at five different substrate concentrations ranging from 0.5 to 8 µmol/l and four different inhibitor concentrations ranging from 20 nmol/l to 1.28 µmol/l for the first-generation aptamers and 10 to 640 nmol/l for the second-generation aptamers. This assay kit employs a HiLyte Fluor 488/QXL 520 FRET peptide that displays greater sensitivity than the EDANS-DABCYL FRET substrate, allowing for measurements at both significantly lower substrate concentrations and lower enzyme input. The reactions were carried out by preincubating 10 nmol/l HIV-1 PR with aptamer RNAs in the selection buffer for 10 minutes at 25 °C. Equal volume of substrate at a 2× concentration was then added to initiate the reactions. The accumulation of the cleaved product was then monitored every 90 seconds for 18 minutes on a Victor 3 plate reader (Perkin Elmer) at 37 °C with excitation at 485 ± 20 nm and emission at 535 ± 25 nm wavelengths. The K_m, V_{max}, and K_i values were determined from nonlinear regression globally fit to the equation for noncompetitive inhibition ($K_i = I/(V_{max}/V_{max}^{app}-1)$ using Prism (Version 5.0b, Graphpad Software) (**Supplementary Figure S1**).

Binding assay with other aspartyl proteases. PR10.1-8E and mutant PR10.1-8E-M9, which does not bind HIV-1 PR, were assayed for their abilities to bind other aspartyl proteases including HIV-2 PR (NIH AIDS Reagent Program, Bethesda, MD) and Cathepsin D (Sigma Aldrich). Each protein preparation was assayed for RNase contamination prior to the binding experiments by incubating ^{32}P-labeled RNA with 200 nmol/l of each protein preparation for 1 hour at 37 °C and separating the resulting species by electrophoresis on an 8% denaturing PAGE. The gel was dried, exposed to a phosphorimager screen for 1 hour, and scanned to visualize RNA degradation (data not shown). The binding reactions were carried out by allowing 1 nmol/l, 10 nmol/l, 100 nmol/l, and 1 µmol/l of each protease to incubate with 1 nmol/l of PR10.1-8E- and

PR10.1-8E-M9-mutant RNA aptamer. The RNA-protein complexes were partitioned and percentage binding was measured as previously described (**Supplementary Figure S2a**).

Inhibition of cathepsin D. A Cathepsin D Assay Kit (Sigma Aldrich) was used to assay the ability of the anti-PR RNA aptamer to inhibit Cathepsin D activity according to manufacturer's protocol. This assay uses an internally quenched fluorescent substrate, MCA-Gly-Lys-Pro-Ile-Leu-Phe-//-Phe-Arg-Leu-Lys(DNP)-D-Arg-NH_2 trifluoroacetate salt that fluoresces upon cleavage with excitation at 328 nm and emission at 393 nm wavelengths. Briefly, 0.1 µg/ml of Cathepsin D was preincubated with up to 1 µmol/l of RNA aptamers in assay buffer for 10 minutes at 37 °C. As a positive control for inhibition, Pepstatin A was used at a final concentration of 200 µg/ml. Cathepsin D substrate was then added at a final concentration of 20 µmol/l to initiate the reactions. The fluorescence intensity was measured every minute for 10 minutes at 37 °C (**Supplementary Figure S2b**).

*Preparation of mutant PR10.*1-8E RNA aptamers. Mutant PR10.1-8E DNA templates were prepared by PCR using specific primers and custom oligonucleotide templates. All primers and oligos were ordered from IDT (Coralville, IA). The primers and oligonucleotides used for each template are provided in the Supplementary Data, **Supplementary Table S1**. A web tool (https://www.random.org) was used to randomly rearrange the nucleotide sequence of PR10.1-8E aptamer to generate the shuffled version, the PR10.1-8E MS mutant, which maintains the original base composition. All templates were purified using Qiagen PCR Purification Kit (Qiagen, Valencia, CA) and confirmed by sequencing in both the forward and reverse directions. Binding affinities of PR10.1-8E mutant aptamers were measured as described above.

Cloning of protease aptamers. Protease aptamers were constructed by generating an aptamer cassette with flanking ribozymes as previously described.[26] Briefly, the hammerhead ribozymes flanking the aptamer sequence were added in order to minimize misfolding of the aptamers. The aptamer-ribozyme cassette was then cloned in a CMV promoter driven RNA expression vector pSilencer4.1-CMV-Puro (Ambion) using XhoI and ApaI restriction sites. Clones were verified by sequencing.

Cells, transfection, and virus production. HEK293T (human embryonic kidney 293T) cells were propagated in Dulbecco's modified Eagle's medium containing 10% fetal bovine serum (Hyclone, Logan, UT) at 37 °C in humidified CO_2 incubator. For transfection, 293T cells were seeded in six-well trays (4×10^5 cells per well) 1 day prior and incubated overnight at 37 °C in CO_2 incubator.

The pNL4-3.Luc.R-E is an envelope deficient reporter plasmid. In addition, its *nef* gene is substituted with a gene encoding Firefly Luciferase. This molecular clone was obtained from the AIDS Research and Reference Reagent program (Division of AIDS, NIAID, NIH).[48,63] The reporter virus was pseudotyped with the vesicular stomatitis virus envelope (VSV-G) using the plasmid pVSV-G (Clontech, Mountain View, CA). HEK 293T cells were cotransfected with pNL4-3.Luc.R-E, pVSV-G and various pSilencer protease aptamer or control plasmids in the following DNA ratio (1.5 µg:1.5 µg:7.5 µg) using calcium–phosphate method (Promega, Madison, WI) according to manufacturer's protocol. Forty-eight hours post-transfection, culture supernatants containing virus were harvested, clarified by centrifugation at 2,000 rpm for 5 minutes, and filtered through 0.45 µm pore size syringe filters to remove residual cell debris. Virus release was determined by measuring p24 levels in the supernatant using HIV-1 p24 antigen capture ELISA assay kit (Advanced Bio-Science Laboratories, Rockville, MD) according to the manufacturer's instructions (**Figure 4**). Transfection efficiency was monitored by measuring luciferase activity in transfected cells using Brightglo-Luciferase assay system (Promega).

Acknowledgments. The authors would like to thank Brad Hall (University of Texas at Austin) for synthesizing the doped RNA pools, Na Li (University of Texas at Austin) and Carlos Garcia (University of Texas at Austin) for their assistance with the initial rounds of selections; Matthew Levy (Albert Einstein College of Medicine) for invaluable advice; Dhivya Ramgalingam (Albert Einstein College of Medicine) for the design of the pSilencer construction and technical help; Kimdar Kemal (Albert Einstein College of Medicine) for technical support; Scott Garforth (Albert Einstein College of Medicine) and William Drosopoulos (Albert Einstein College of Medicine) for critically reading the manuscript; and the Programme EVA Centre for AIDS Reagents, NIBSC, UK for providing recombinant HIV-1 PR (EVA630). S.D. was supported by an institutional NIH AIDS Training grant T32 AI007501 and a NIH MARC fellowship F31-GM78730. The research described in this report was supported by NIH grants P01 AI061797 and R37 AI030861 to V.R.P. S.D. performed a majority of the experimental work described in this manuscript, prepared the draft of the manuscript and all the figures except Figure 4. A.G. performed the transfections and virus production assays. V.R.P. conceived of the project, designed, and supervised the overall approach and helped generate the final manuscript. The author(s) declare that they have no competing interests.

Supplementary material

Figure S1. Analysis of the mode of inhibition of the anti-PR RNA aptamers.
Figure S2. Specificity of anti-PR RNA aptamers.
Figure S3. Cell-associated and virus-associated p24.
Figure S4. Effect of anti-PR aptamers on the processing of viral proteins.
Figure S5. Infectivity of progeny virion particles produced in the presence of aptamers.
Table S1. Preparation of the PR10.1-8E mutant aptamer templates.
Table S2. Binding affinities of mutant PR10.1-8E RNA aptamers.

1. Gottlinger, HG, Sodroski, JG and Haseltine, WA (1989). Role of capsid precursor processing and myristoylation in morphogenesis and infectivity of human immunodeficiency virus type-1. *Proc Natl Acad Sci USA* **86**: 5781–5785.
2. Seelmeier, S, Schmidt, H, Turk, V and Vonderhelm, K (1988). Human immunodeficiency virus has an aspartic-type protease that can be inhibited by pepstatin-A. *Proc Natl Acad Sci USA* **85**: 6612–6616.
3. Wiegers, K, Rutter, G, Kottler, H, Tessmer, U, Hohenberg, H and Kräusslich, HG (1998). Sequential steps in human immunodeficiency virus particle maturation revealed by alterations of individual Gag polyprotein cleavage sites. *J Virol* **72**: 2846–2854.
4. Kaplan, AH, Manchester, M and Swanstrom, R (1994). The activity of the protease of human immunodeficiency virus type 1 is initiated at the membrane of infected cells before the release of viral proteins and is required for release to occur with maximum efficiency. *J Virol* **68**: 6782–6786.
5. McQuade, TJ, Tomasselli, AG, Liu, L, Karacostas, V, Moss, B, Sawyer, TK *et al.* (1990). A synthetic HIV-1 protease inhibitor with antiviral activity arrests HIV-like particle maturation. *Science* **247**: 454–456.
6. Schätzl, H, Gelderblom, HR, Nitschko, H and von der Helm, K (1991). Analysis of non-infectious HIV particles produced in presence of HIV proteinase inhibitor. *Arch Virol* **120**: 71–81.
7. Wlodawer, A and Vondrasek, J (1998). Inhibitors of HIV-1 protease: a major success of structure-assisted drug design. *Annu Rev Biophys Biomol Struct* **27**: 249–284.
8. Vacca, JP and Condra, JH (1997). Clinically effective HIV-1 protease inhibitors. *Drug Discov Today* **2**: 261–272.
9. Palella, FJ Jr, Delaney, KM, Moorman, AC, Loveless, MO, Fuhrer, J, Satten, GA *et al.* (1998). Declining morbidity and mortality among patients with advanced human immunodeficiency virus infection. HIV Outpatient Study Investigators. *N Engl J Med* **338**: 853–860.
10. Hammer, SM, Katzenstein, DA, Hughes, MD, Gundacker, H, Schooley, RT, Haubrich, RH *et al.* (1996). A trial comparing nucleoside monotherapy with combination therapy in HIV-infected adults with CD4 cell counts from 200 to 500 per cubic millimeter. AIDS Clinical Trials Group Study 175 Study Team. *N Engl J Med* **335**: 1081–1090.
11. Hoetelmans, RM, Meenhorst, PL, Mulder, JW, Burger, DM, Koks, CH and Beijnen, JH (1997). Clinical pharmacology of HIV protease inhibitors: focus on saquinavir, indinavir, and ritonavir. *Pharm World Sci* **19**: 159–175.
12. Weber, IT (1990). Comparison of the crystal structures and intersubunit interactions of human immunodeficiency and Rous sarcoma virus proteases. *J Biol Chem* **265**: 10492–10496.
13. Gustchina, A and Weber, IT (1991). Comparative analysis of the sequences and structures of HIV-1 and HIV-2 proteases. *Proteins* **10**: 325–339.
14. Boggetto, N and Reboud-Ravaux, M (2002). Dimerization inhibitors of HIV-1 protease. *Biol Chem* **383**: 1321–1324.
15. Zhang, ZY, Poorman, RA, Maggiora, LL, Heinrikson, RL and Kézdy, FJ (1991). Dissociative inhibition of dimeric enzymes. Kinetic characterization of the inhibition of HIV-1 protease by its COOH-terminal tetrapeptide. *J Biol Chem* **266**: 15591–15594.
16. Schramm, HJ, de Rosny, E, Reboud-Ravaux, M, Büttner, J, Dick, A and Schramm, W (1999). Lipopeptides as dimerization inhibitors of HIV-1 protease. *Biol Chem* **380**: 593–596.
17. Tuerk, C and Gold, L (1990). Systematic evolution of ligands by exponential enrichment: RNA ligands to bacteriophage T4 DNA polymerase. *Science* **249**: 505–510.
18. Ellington, AD and Szostak, JW (1990). *In vitro* selection of RNA molecules that bind specific ligands. *Nature* **346**: 818–822.
19. Somasunderam, A, Ferguson, MR, Rojo, DR, Thiviyanathan, V, Li, X, O'Brien, WA *et al.* (2005). Combinatorial selection, inhibition, and antiviral activity of DNA thioaptamers targeting the RNase H domain of HIV-1 reverse transcriptase. *Biochemistry* **44**: 10388–10395.
20. Tuerk, C, Macdougal, S and Gold, L (1992). RNA pseudoknots that inhibit human-immunodeficiency-virus type-1 reverse-transcriptase. *Proc Natl Acad Sci USA* **89**: 6988–6992.
21. Allen, P, Worland, S and Gold, L (1995). Isolation of high-affinity RNA ligands to HIV-1 integrase from a random pool. *Virology* **209**: 327–336.
22. Yamamoto, R, Toyoda, S, Viljanen, P, Machida, K, Nishikawa, S, Murakami, K *et al.* (1995). *In vitro* selection of RNA aptamers that can bind specifically to Tat protein of HIV-1. *Nucleic Acids Symp Ser* **34**: 145–146.
23. Duconge, F and Toulme, JJ (1999). In vitro selection identifies key determinants for loop-loop interactions: RNA aptamers selective for the TAR RNA element of HIV-1. *RNA-Publ RNA Soc* **5**: 1605–1614.
24. Giver, L, Bartel, D, Zapp, M, Pawul, A, Green, M and Ellington, AD (1993). Selective optimization of the Rev-binding element of HIV-1. *Nucleic Acids Res* **21**: 5509–5516.
25. Jensen, KB, Atkinson, BL, Willis, MC, Koch, TH and Gold, L (1995). Using *in vitro* selection to direct the covalent attachment of human immunodeficiency virus type 1 Rev protein to high-affinity RNA ligands. *Proc Natl Acad Sci USA* **92**: 12220–12224.
26. Ramalingam, D, Duclair, S, Datta, SA, Ellington, A, Rein, A and Prasad, VR (2011). RNA aptamers directed to human immunodeficiency virus type 1 Gag polyprotein bind to the matrix and nucleocapsid domains and inhibit virus production. *J Virol* **85**: 305–314.
27. Lochrie, MA, Waugh, S, Pratt, DG Jr, Clever, J, Parslow, TG and Polisky, B (1997). *In vitro* selection of RNAs that bind to the human immunodeficiency virus type-1 gag polyprotein. *Nucleic Acids Res* **25**: 2902–2910.
28. Kim, SJ, Kim, MY, Lee, JH, You, JC and Jeong, S (2002). Selection and stabilization of the RNA aptamers against the human immunodeficiency virus type-1 nucleocapsid protein. *Biochem Biophys Res Commun* **291**: 925–931.
29. Sayer, N, Ibrahim, J, Turner, K, Tahiri-Alaoui, A and James, W (2002). Structural characterization of a 2'F-RNA aptamer that binds a HIV-1 SU glycoprotein, gp120. *Biochem Biophys Res Commun* **293**: 924–931.
30. Zhou, J, Swiderski, P, Li, H, Zhang, J, Neff, CP, Akkina, R *et al.* (2009). Selection, characterization and application of new RNA HIV gp 120 aptamers for facile delivery of Dicer substrate siRNAs into HIV infected cells. *Nucleic Acids Res* **37**: 3094–3109.
31. Sekiya, S, Nishikawa, F, Fukuda, K and Nishikawa, S (2003). Structure/function analysis of an RNA aptamer for hepatitis C virus NS3 protease. *J Biochem* **133**: 351–359.
32. Povsic, TJ, Vavalle, JP, Alexander, JH, Aberle, LH, Zelenkofske, SL, Becker, RC *et al.*; RADAR Investigators. (2014). Use of the REG1 anticoagulation system in patients with acute coronary syndromes undergoing percutaneous coronary intervention: results from the phase II RADAR-PCI study. *EuroIntervention* **10**: 431–438.
33. Joshi, P and Prasad, VR (2002). Potent inhibition of human immunodeficiency virus type 1 replication by template analog reverse transcriptase inhibitors derived by SELEX (systematic evolution of ligands by exponential enrichment). *J Virol* **76**: 6545–6557.
34. Chaloin, L, Lehmann, MJ, Sczakiel, G and Restle, T (2002). Endogenous expression of a high-affinity pseudoknot RNA aptamer suppresses replication of HIV-1. *Nucleic Acids Res* **30**: 4001–4008.
35. Joshi, PJ, North, TW and Prasad, VR (2005). Aptamers directed to HIV-1 reverse transcriptase display greater efficacy over small hairpin RNAs targeted to viral RNA in blocking HIV-1 replication. *Mol Ther* **11**: 677–686.
36. Kolb, G, Reigadas, S, Castanotto, D, Faure, A, Ventura, M, Rossi, JJ *et al.* (2006). Endogenous expression of an anti-TAR aptamer reduces HIV-1 replication. *RNA Biol* **3**: 150–156.
37. Neff, CP, Zhou, J, Remling, L, Kuruvilla, J, Zhang, J, Li, H *et al.* (2011). An aptamer-siRNA chimera suppresses HIV-1 viral loads and protects from helper CD4(+) T cell decline in humanized mice. *Sci Transl Med* **3**: 66ra6.
38. Lange, MJ, Sharma, TK, Whatley, AS, Landon, LA, Tempesta, MA, Johnson, MC *et al.* (2012). Robust suppression of HIV replication by intracellularly expressed reverse transcriptase aptamers is independent of ribozyme processing. *Mol Ther* **20**: 2304–2314.
39. Rossi, JJ, June, CH and Kohn, DB (2007). Genetic therapies against HIV. *Nat Biotechnol* **25**: 1444–1454.
40. Kitchen, SG, Shimizu, S and An, DS (2011). Stem cell-based anti-HIV gene therapy. *Virology* **411**: 260–272.
41. Mitsuyasu, RT, Merigan, TC, Carr, A, Zack, JA, Winters, MA, Workman, C *et al.* (2009). Phase 2 gene therapy trial of an anti-HIV ribozyme in autologous CD34+ cells. *Nat Med* **15**: 285–292.
42. Morgan, RA, Walker, R, Carter, CS, Natarajan, V, Tavel, JA, Bechtel, C *et al.* (2005). Preferential survival of CD4+ T lymphocytes engineered with anti-human immunodeficiency virus (HIV) genes in HIV-infected individuals. *Hum Gene Ther* **16**: 1065–1074.
43. Levine, BL, Humeau, LM, Boyer, J, MacGregor, RR, Rebello, T, Lu, X *et al.* (2006). Gene transfer in humans using a conditionally replicating lentiviral vector. *Proc Natl Acad Sci USA* **103**: 17372–17377.
44. Tebas, P, Stein, D, Tang, WW, Frank, I, Wang, SQ, Lee, G *et al.* (2014). Gene editing of CCR5 in autologous CD4 T cells of persons infected with HIV. *N Engl J Med* **370**: 901–910.
45. Li, N, Wang, YX, Pothukuchy, A, Syrett, A, Husain, N, Gopalakrisha, S *et al.* (2009). Aptamers that recognize drug-resistant HIV-1 reverse transcriptase (vol 36, pg 6739, 2008). *Nucleic Acids Res* **37**: 5236–5236.
46. Zuker, M (2003). Mfold web server for nucleic acid folding and hybridization prediction. *Nucleic Acids Res* **31**: 3406–3415.
47. Liaudet-Coopman, E, Beaujouin, M, Derocq, D, Garcia, M, Glondu-Lassis, M, Laurent-Matha, V *et al.* (2006). Cathepsin D: newly discovered functions of a long-standing aspartic protease in cancer and apoptosis. *Cancer Lett* **237**: 167–179.
48. He, J, Choe, S, Walker, R, Di Marzio, P, Morgan, DO and Landau, NR (1995). Human immunodeficiency virus type 1 viral protein R (Vpr) arrests cells in the G2 phase of the cell cycle by inhibiting p34cdc2 activity. *J Virol* **69**: 6705–6711.
49. Scherer, LJ, Frank, R and Rossi, JJ (2007). Optimization and characterization of tRNA-shRNA expression constructs. *Nucleic Acids Res* **35**: 2620–2628.
50. Lee, NS, Dohjima, T, Bauer, G, Li, H, Li, MJ, Ehsani, A *et al.* (2002). Expression of small interfering RNAs targeted against HIV-1 rev transcripts in human cells. *Nat Biotechnol* **20**: 500–505.
51. Perryman, AL, Lin, JH and McCammon, JA (2004). HIV-1 protease molecular dynamics of a wild-type and of the V82F/I84V mutant: Possible contributions to drug resistance and a potential new target site for drugs (vol 13, pg 1108, 2004). *Protein Sci* **13**: 1434–1434.
52. Hornak, V and Simmerling, C (2007). Targeting structural flexibility in HIV-1 protease inhibitor binding. *Drug Discov Today* **12**: 132–138.
53. Navia, MA, Fitzgerald, PM, McKeever, BM, Leu, CT, Heimbach, JC, Herber, WK *et al.* (1989). Three-dimensional structure of aspartyl protease from human immunodeficiency virus HIV-1. *Nature* **337**: 615–620.
54. Wlodawer, A, Miller, M, Jaskólski, M, Sathyanarayana, BK, Baldwin, E, Weber, IT *et al.* (1989). Conserved folding in retroviral proteases: crystal structure of a synthetic HIV-1 protease. *Science* **245**: 616–621.

55. Vondrasek, J and Wlodawer, A (2002). HIVdb: a database of the structures of human immunodeficiency virus protease. *Proteins* **49**: 429–431.
56. Nicholson, LK, Yamazaki, T, Torchia, DA, Grzesiek, S, Bax, A, Stahl, SJ *et al.* (1995). Flexibility and function in HIV-1 protease. *Nat Struct Biol* **2**: 274–280.
57. Freedberg, DI, Ishima, R, Jacob, J, Wang, YX, Kustanovich, I, Louis, JM *et al.* (2002). Rapid structural fluctuations of the free HIV protease flaps in solution: relationship to crystal structures and comparison with predictions of dynamics calculations. *Protein Sci* **11**: 221–232.
58. Ishima, R, Freedberg, DI, Wang, YX, Louis, JM and Torchia, DA (1999). Flap opening and dimer-interface flexibility in the free and inhibitor-bound HIV protease, and their implications for function. *Structure* **7**: 1047–1055.
59. Bowman, MJ, Byrne, S and Chmielewski, J (2005). Switching between allosteric and dimerization inhibition of HIV-1 protease. *Chem Biol* **12**: 439–444.
60. Rezacova, P, Brynda, J, Lescar, J, Fabry, M, Horejsi, M, Sieglova, I *et al.* (2005). Crystal structure of a cross-reaction complex between an anti-HIV-1 protease antibody and an HIV-2 protease peptide. *J Struct Biol* **149**: 332–337.
61. Huang, L, Sayer, JM, Swinford, M, Louis, JM and Chen, C (2009). Modulation of human immunodeficiency virus type 1 protease autoprocessing by charge properties of surface residue 69. *J Virol* **83**: 7789–7793.
62. Piasecki, SK, Hall, B and Ellington, AD (2009). Nucleic acid pool preparation and characterization. *Methods Mol Biol* **535**: 3–18.
63. Connor, RI, Chen, BK, Choe, S and Landau, NR (1995). Vpr is required for efficient replication of human immunodeficiency virus type-1 in mononuclear phagocytes. *Virology* **206**: 935–944.

Supplementary Information accompanies this paper on the Molecular Therapy–Nucleic Acids website (http://www.nature.com/mtna)